Projected Climate Change in the Hindu Kush–Himalayan Region By Using the High-resolution Regional Climate Model PRECIS

Author(s): Ashwini Kulkarni, Savita PatwardhanK. Krishna Kumar, Karamuri Ashok, and Raghavan Krishnan

Projected Climate Change in the Hindu Kush–Himalayan Region By Using the High-resolution Regional Climate Model PRECIS

Ashwini Kulkarni*, Savita Patwardhan, K. Krishna Kumar, Karamuri Ashok, and Raghavan Krishnan
* Corresponding author: ashwini@tropmet.res.in
Indian Institute of Tropical Meteorology, Pune, India

Open access article: please credit the authors and the full source.

The Hindu Kush–Himalayan (HKH) region is characterized by a variety of climatic conditions from tropical to alpine. It has been documented that the rates of warming in the HKH region are significantly higher than the global average and that the warming is occurring at much higher rates in the high-altitude regions than in the low-altitude regions. Mountainous environments are considered sensitive indicators of climate change. Hence this study examined the potential impact of global warming on the HKH region by applying Hadley Centre's high-resolution regional climate model PRECIS (Providing Regional Climates for Impact Studies) to 3 subregions: the western, central, and eastern Himalaya. The physical mechanisms that drive warming are different for the 3 regions, and the western Himalaya has 2 major rainy seasons, whereas the central and eastern Himalaya have only one. This study therefore focused on the common rainy season (June–September), during which all 3 regions receive the highest proportion of their annual rainfall. The 3 PRECIS simulations that correspond to the Intergovernmental Panel on Climate Change's A1B emissions scenario were carried out for a continuous period from 1961 to 2098. They were validated with high-resolution (0.25° latitude × 0.25° longitude) data provided by the Asian Precipitation—Highly Resolved Observational Data Integration Towards Evaluation of the Water Resources (APHRODITE) project and by the US National Centers for Environmental Prediction and National Center for Atmospheric Research (NCEP/NCAR) reanalysis data. The model was reasonably effective in simulating the monsoon climate over the HKH region. The climate projections were examined over the short (2011–2040), medium (2041–2070), and long term (2071–2098). The model projections indicate that significant warming will occur throughout the HKH region toward the end of the 21st century. Summer monsoon precipitation is expected to be 20–40% higher in 2071–2098 than it was in the baseline period (1961–1990). The 3 Quantifying Uncertainty in Model Predictions simulations show large differences in projections in the western Himalaya.

Keywords: Climate change; monsoon; regional climate model simulated projections; Hindu Kush–Himalayas.

Introduction

The Hindu Kush–Himalayan (HKH) region is believed to be a hotspot of climate change (IPCC 2007), but not much is known in detail about the region. Rising temperatures are expected to have a greater impact here than elsewhere in the world because they can disturb the fine equilibrium that governs how the vast reserves of snow, ice, and water in the high mountains provide water to rivers downstream. Changes in temperature are also likely to affect the hydrological cycle and have global implications (IPCC 2007). Bolch et al (2012) have shown that most Himalayan glaciers are losing mass at a rate similar to glaciers elsewhere; however, there are indications that mass gain in the Karakoram region may remain stable. Dramatic changes in total runoff are unlikely.

The rates of warming in the HKH region are significantly higher than the global average of 0.74°C over the past 100 years (Du et al 2004; IPCC 2007). The rates in the western Himalaya (WH), eastern Himalaya (EH), and the plains of the Ganges basin over the past 25 years have been lower (0.01–0.03°C per year), and those for the central Himalaya (CH), especially Nepal, and the Tibetan Plateau appear, based on limited station data, to have been considerably higher (0.04–0.09°C per year for Nepal and 0.03–0.07°C per year for Tibet). Measurements in Nepal and Tibet also indicate that warming is occurring at much higher rates in high-altitude regions than at low altitudes (Shrestha et al 1999). This rapid warming has had a profound effect on the Himalayan environment, perhaps most visibly in the rapid retreat of Himalayan glaciers and diminishing snow fields (Dyurgerov and Meier 2005).

The rise in temperature shows strong seasonality (time when the peak values occur). The winter mean and maximum temperatures show significant increases, whereas mean and minimum summer temperatures show consistent decline in the Karakoram and HKH mountains of the upper Indus basin (Fowler and Archer 2006;

Forsythe et al 2012). This cooling is likely a key factor in the positive glacial mass balance in the WH found by several recent studies (eg Jacob et al 2012; Yao et al 2012). However, average annual temperatures show a consistent warming across the HKH region; hence, this study considered the projected changes in annual average temperatures.

Total rainfall has not shown any distinct trends related to climate change. Shrestha and Devkota (2010) investigated the likely changes in mean seasonal and annual temperatures as well as precipitation across the EH under a warmer climate, by using the high-resolution regional climate model Providing Regional Climates for Impact Studies (PRECIS). Their analysis shows a likely rise, under the Intergovernmental Panel on Climate Change's B2 (A2) emissions scenarios, of 2.9°C (4.3°C) in mean annual temperature by the late 21st century. The expected change in precipitation in the EH is +13% (+34%) under the B2 (A2) scenario by the late 21st century.

As Xu et al (2009) underlines, climate change is affecting the temperatures and amount of snow and ice in the Himalaya as well as rainfall patterns in the densely populated downstream regions of Asia, which would have enormous significance for the livelihoods and wellbeing of the people of the region. Climate change will have environmental and social impacts that will likely increase uncertainty about water supplies and agricultural production for people across Asia. The cascading effects of rising temperatures and the loss of ice and snow in the region are already affecting water availability (amount and seasonality), biodiversity (survival of endemic species and predator–prey relations), ecosystem boundaries (tree-line movements and high-elevation ecosystem changes), and global feedbacks (monsoonal shifts and loss of soil carbon) (Xu et al 2009). Poor people in mountain regions have made the least contribution to climate change in terms of greenhouse gas emissions; however, they will suffer disproportionately from the negative impact of climate change.

This article attempts to reconcile existing reanalyzed and satellite observations to glean new information on climate change in the HKH region. Due to the lack of long-term observed data at sufficient locations and the lack of model outputs on finer spatial scales, not much work has been done on climate change impact in this region. The most important objective of this work is to discuss climate change projections for the 3 HKH subregions by using the outputs from the PRECIS model. The downscaling strategy involves the introduction of uncertainties associated with model physics (Stainforth et al 2005). The model outputs have been validated with the newly developed high-resolution observed data set described below. We concentrated on projected changes in seasonal (June–September) rainfall and annual average temperature in the 3 subregions. The WH experiences 2

rainy seasons, February–April and June–September. Because the focus of this study is on the entire HKH region, we considered the June–September rainy season, which is common to all 3 subregions.

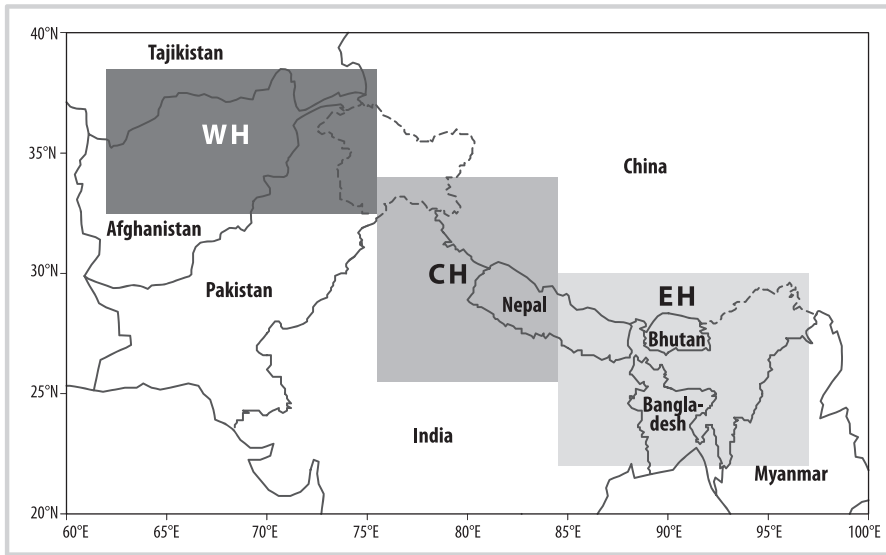## Material and methods

Data

The long-term pattern of precipitation in this region is not well known due to a lack of long-term observations even at spatial scales of a few tens of kilometers (Grabs and Pokhrel 1992; Fujita et al 1997; Shrestha et al 1999). Small-scale studies are necessary because the complex terrain can introduce significant differences in climate, even across short distances. Most existing rain-gauge networks, especially in complex mountainous areas, are not dense enough to fulfill this requirement. However, the recently introduced Asian Precipitation – Highly Resolved Observational Data Integration Towards the Evaluation of Water Resources (APHRODITE) project (Yatagai et al 2009, 2012) makes available a lengthy daily gridded high-resolution data set that was prepared by collecting rain-gauge observational data from thousands of stations across Asia. This data set (APHRO_V1003R1) is a long-term (1951–2007) continental-scale product that contains a dense network of daily rain-gauge data for Asia, including the Himalaya and mountainous areas in the Middle East. APHRO_V1003R1 data sets for Monsoon Asia, Russia, and the Middle East (on $0.5° \times 0.5°$ and $0.25° \times 0.25°$ latitude/longitude grids) are available at http://www.chikyu.ac.jp/precip/. For this analysis we used the $0.25° \times 0.25°$ data. We validated these data for the Indian region by comparing the seasonal monsoon rainfall with data sets from the India Meteorological Department, Global Precipitation Analysis, and the Climate Prediction Center's Merged Analysis of Precipitation (Patwardhan 2012). APHRODITE is also being increasingly used for operational climate applications such as extreme drought and flood forecasting in East Asia (Sohn et al 2011). This data set bridges the gap in long-period observed station data for the HKH region.

Stations in the WH are quite sparse compared with the CH and EH (Yatagai et al 2012); hence, if the spatial interpolation applied by the APHRODITE algorithm does not compensate by reproducing orographic precipitation enhancement then precipitation estimates in this subregion will be differentially biased compared with the other 2 regions.
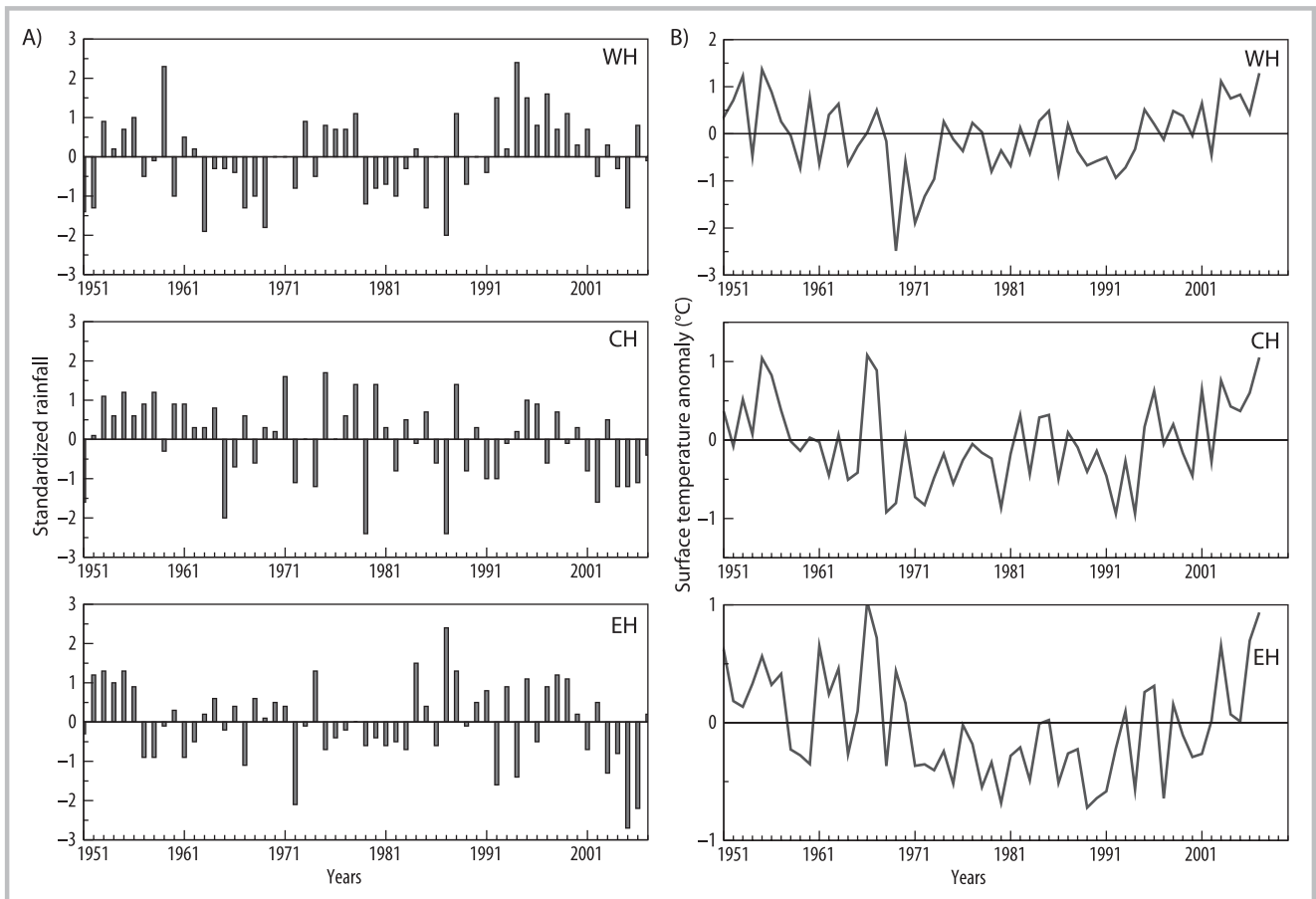
This study used the following data:

1. APHRODITE rainfall data at $0.25° \times 0.25°$ resolution for 1951–2007.
2. Gridded monthly surface air temperature data for 1948–2010 at $2.5° \times 2.5°$ resolution from the US National Centers for Environmental Prediction and National Center for Atmospheric Research (NCEP/

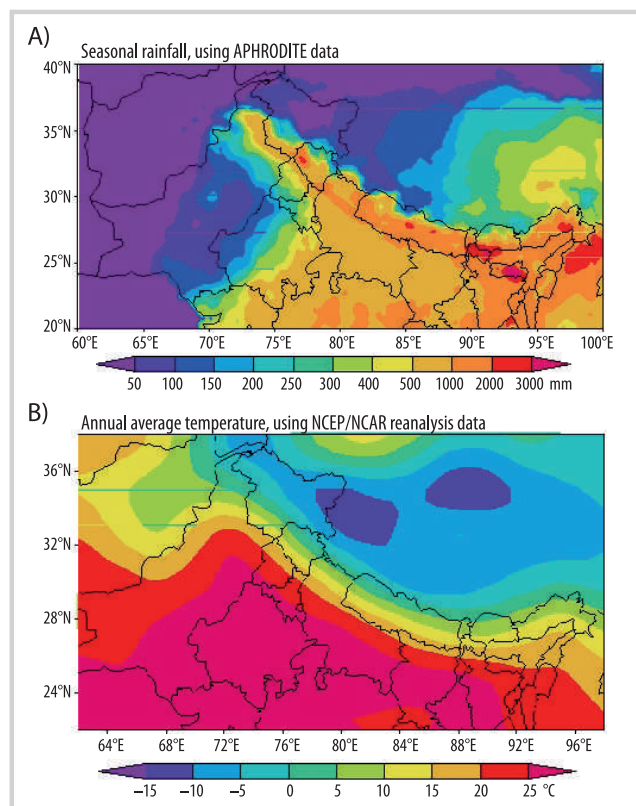**FIGURE 1** The Hindu Kush–Himalayan region considered in this analysis. The region was divided into 3 subregions: WH, 62–75.5°E, 32.5–38.5°N; CH, 75.5–84.5°E, 25.5–34°N; and EH, 84.5–97°E, 22–30°N. (Map by authors)

FIGURE 2 (A) Interannual variability of standardized June through September (JJAS) rainfall and (B) anomalies of annual average temperature (°C), 1951–2007, in the WH, CH, and EH.

FIGURE 3 (A) Seasonal (June–September) rainfall (mm) based on APHRODITE data; (B) annual average temperature (°C) based on NCEP/NCAR reanalysis data for 1961–1990.

NCAR) reanalysis (for details refer to Kalnay et al 1996).

3. PRECIS data for 3 perturbed physics ensembles from the Quantifying Uncertainty in Model Predictions (QUMP) project.

PRECIS is an atmospheric and land surface model of limited area and high resolution that is locatable over any part of the globe. Dynamic flow, the atmospheric sulfur cycle, clouds and precipitation, radiative processes, the land surface, and the deep soil are all described, and boundary conditions are required at the limits of the model's domain. The basic aspects explicitly handled by the model are described in Jones et al (2004). The lateral boundary conditions required to drive the regional climate model are taken from the perturbed physics ensembles simulations of HadCM3, the global climate model of the Met Office Hadley Centre in the United Kingdom.

Perturbed physics ensembles

Simulations from a 17-member perturbed physics ensemble produced by using HadCM3 under the QUMP project of the Hadley Centre have been used as lateral boundary conditions for 138-year simulations of the PRECIS regional climate model. The perturbed physics approach was developed in response to the call for better

quantification of uncertainties in climate projections (see chapter 14 of the Third Assessment report of IPCC 2001). A significant amount of perturbed physics experimentation has been done with HadCM3 and variants, starting with the work of Murphy et al (2004) and Stainforth et al (2005).

The QUMP simulations comprise 17 versions of the fully coupled version of HadCM3, 1 with the standard parameter setting and 16 in which 29 of the atmosphere component parameters are simultaneously perturbed (Collins et al 2006). The lateral boundary conditions for 3 QUMP simulations (Q0, Q1, and Q14) for the Intergovernmental Panel on Climate Change's A1B emissions scenario (IPCC 2001) were made available by the Hadley Centre. These 3 QUMP runs were carried out at Indian Institute of Tropical Meteorology in Pune, India, for the period 1961–2098 for the area that stretches from longitude 56.77°–103°E and latitude 1.5°–38°N, and were used to generate an ensemble of future climate change scenarios for the HKH region. These simulations were made at 50×50 km horizontal resolution. The daily precipitation and surface air temperature from the QUMP simulations were analyzed to develop high-resolution regional climate change scenarios to study the impact of global warming on the HKH region climate. The impacts were studied for 3 time periods: 2011–2040, 2041–2070, and 2071–2098. The likely changes in precipitation and temperature were tested for their significance by applying the standard Student's t-test. The statistical significance of the trend in area-averaged time series was tested by using the nonparametric Mann-Kendall test (Mann 1945).

Results and discussion

Current climate variability

Observed rainfall and temperature variability: The HKH region's division into 3 subregions (WH, 62–75.5°E and 32.5–38.5°N; CH, 75.5–84.5°E and 25.5–34°N; EH, 84.5–97°E and 22–30°N; see Figure 1) is primarily based on climate and topography. The observed mean rainfall for June through September for 1961–1990 was 86, 546, and 1042 mm, and the coefficient of variations (defined as [standard deviation / mean] $\times$ 100) is 18, 16, and 9% for the WH, CH, and EH, respectively; and mean annual temperatures were 9.9, 8.9, and 13.6°C, respectively. To examine the interannual variability of seasonal (June–September) rainfall, a long time series (1951–2007) of seasonal rainfall was prepared for these 3 regions by using APHRODITE data. The total June–September rainfall over grids that lie in these 3 regions was averaged for every year. The mean rainfall was subtracted from each value and divided by the standard deviation to compute standardized time series for 1951–2007. The standardized rainfall series over the WH, CH, and EH are depicted in

FIGURE 4   Annual cycles of surface air temperature and rainfall in the WH, CH, and EH simulated by 3 QUMP experiments, Q0 (red), Q1 (green), and Q14 (blue), their multimodel ensemble (MME; dashed magenta line), and the APHRODITE rainfall values and NCEP reanalysis temperature values (black, observed) for 1961–1990.
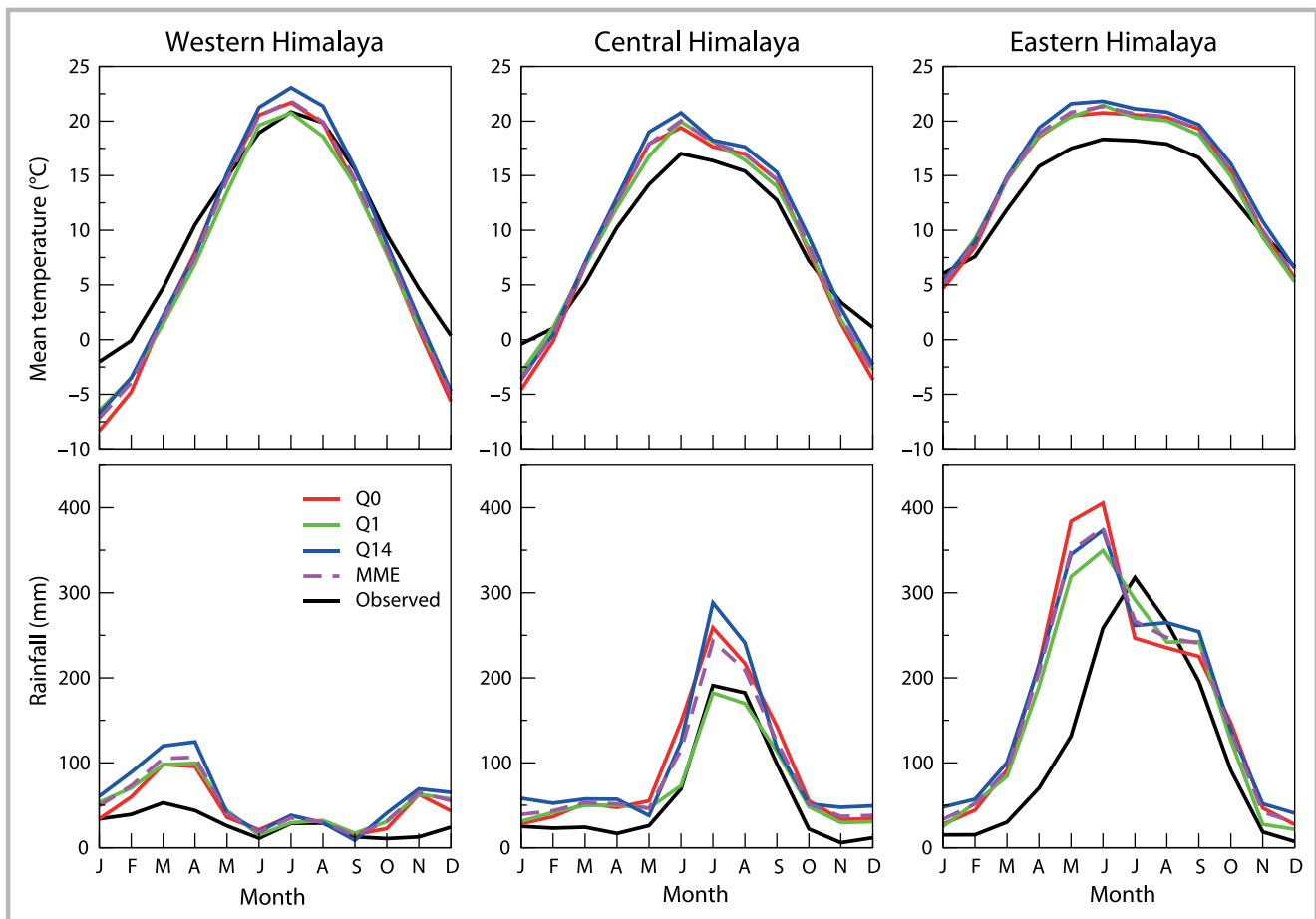

Figure 2A. All 3 time series are highly random and do not show any significant trend. However, it is well observed that the seasonal rainfall in the CH and EH declined substantially after 2000.

The anomaly time series of annual average surface air temperature over the 3 regions are shown in Figure 2B. These time series were prepared by using monthly surface air temperature data from the NCEP/NCAR reanalysis data set for 1948–2010. Temperatures were quite cool from 1970–1990 in all 3 regions; after the 1990s, they increased, although not to a statistically significant degree. Warming has been more rapid in the CH than in the EH and WH.
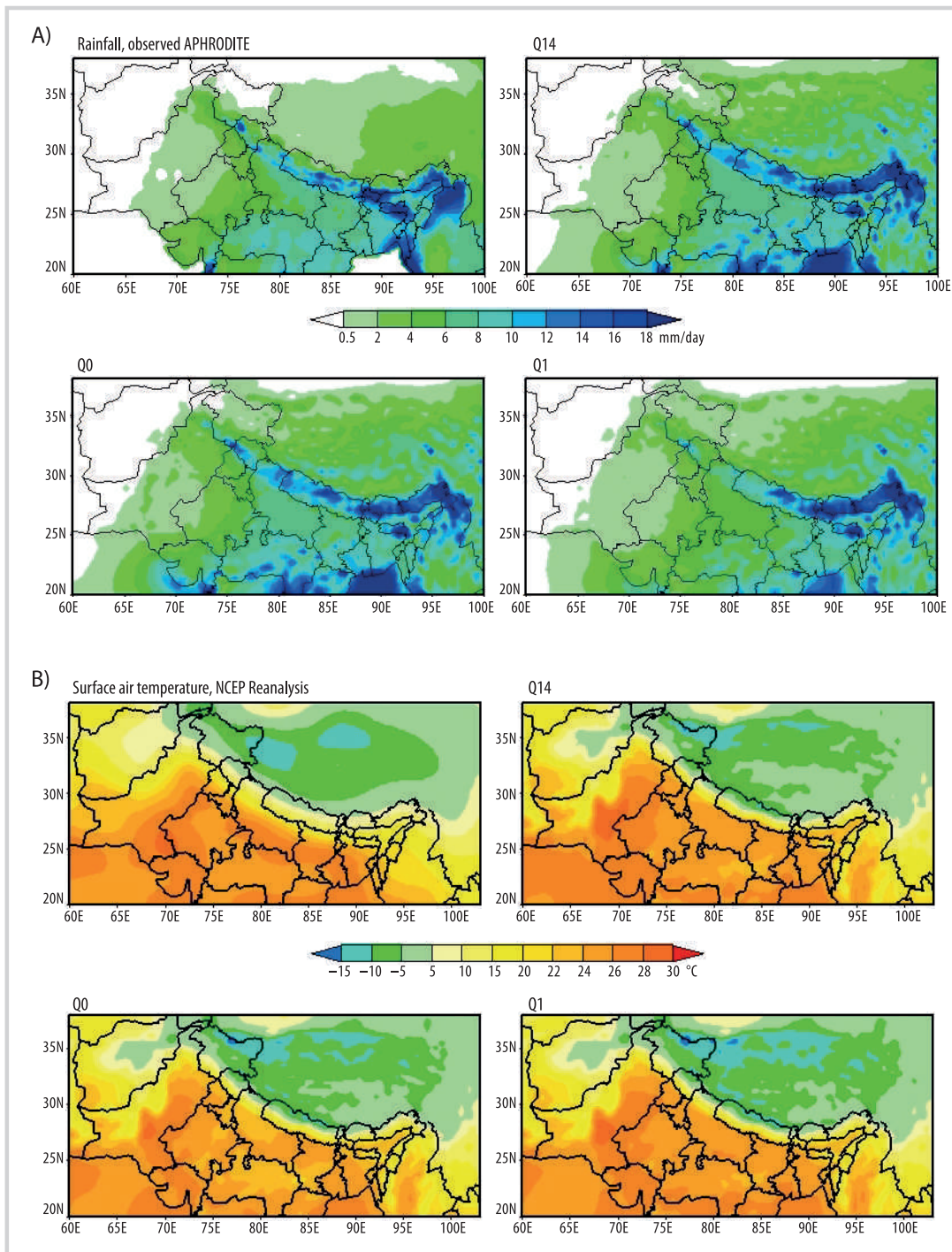
The spatial patterns of observed APHRODITE seasonal rainfall data and NCEP/NCAR reanalysis annual average temperature data are shown in Figure 3A and B, respectively. These composites were prepared based on data for 1961–1990 for validation of model simulations. In the WH, rainfall ranged from 50–500 mm. The levels were lowest in the northwestern parts of the WH and increased from northwest to southeast. In the CH, rainfall ranged between 500 and 1000 mm, and in some parts exceeded

1000 mm, whereas, in the EH, it was more than 1000 mm. In northern parts of Bangladesh and far northeastern parts of India, rainfall exceeded 3000 mm. Annual average temperatures (Figure 3B) decreased from south to north over the HKH region. The QUMP simulations were validated with these patterns, as shown below, to examine their ability to reproduce the current climate.

Model-simulated rainfall and temperature variability: The high-resolution regional simulations generated by using PRECIS, with lateral boundary conditions from QUMP simulations, were studied in detail to evaluate the model's effectiveness in representing the regional climatological features in terms of both annual cycles and spatial patterns. This was the first time that QUMP simulations were used for the HKH region.

Regarding annual cycles, the monthly mean temperature and rainfall simulated by the 3 scenarios based for 1961–1990 for the 3 regions as well as the observed rainfall (from APHRODITE) and temperature (from the NCEP reanalysis) are depicted in Figure 4. In all 3 regions, all 3 QUMP runs simulated the shape of the
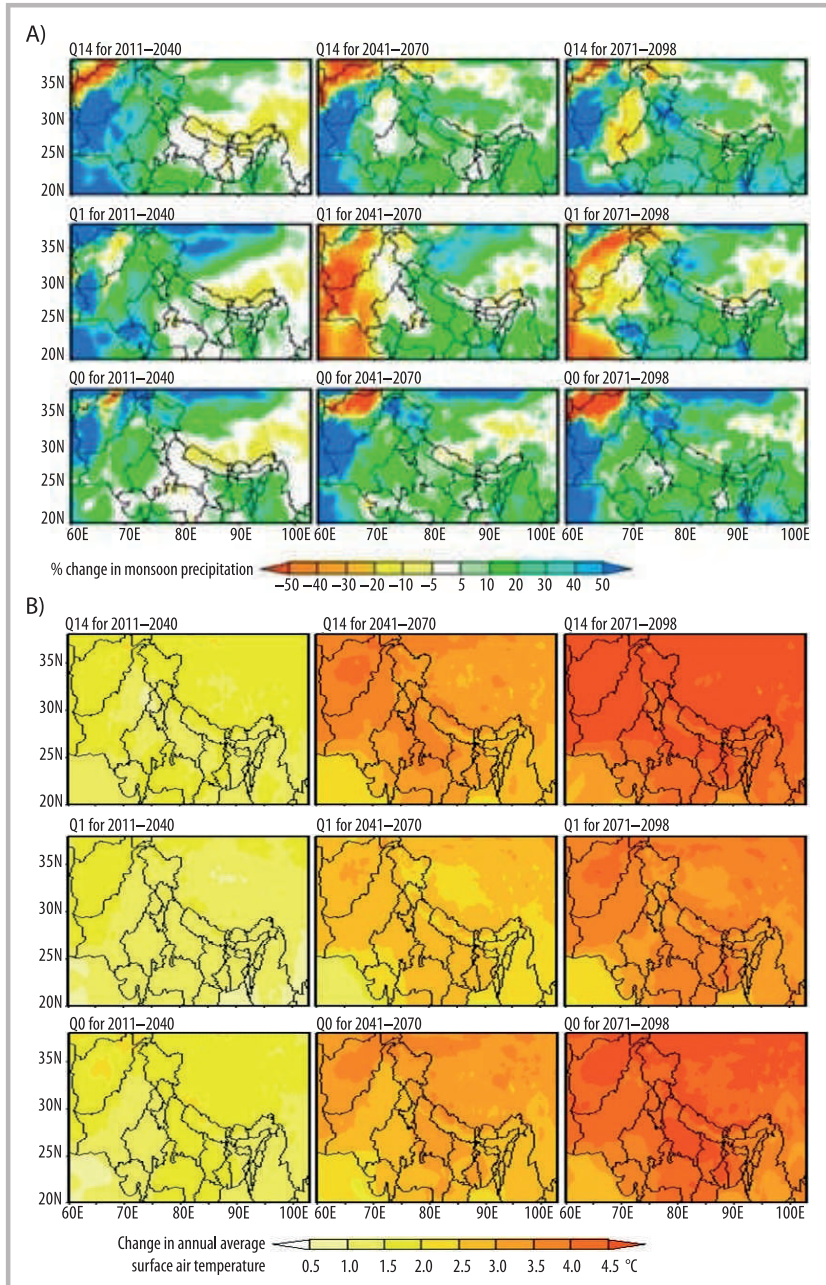
FIGURE 5 (A) Composite seasonal (June–September) monsoon rainfall (mm/d) simulated by 3 QUMP runs compared with the observed APHRODITE values for 1961–1990; (B) composite annual average surface air temperature (°C) simulated by 3 QUMP runs compared with the observed NCEP reanalysis values for 1961–1990.

annual cycle of surface air temperature reasonably well; however, they exhibited a cold bias in winter. The temperatures for the monsoon season were well simulated. The mean temperatures were not corrected for the lapse rate effect of the differences in mean elevations in the various data sets used in the analysis.

The shape of the annual rainfall cycle was well captured by all the simulations for the WH and CH; however, for the EH, the maximum rainfall was simulated 2 months ahead, in May and June. For all 3 regions, a wet bias was exhibited. For the WH, a large wet bias of 20 mm was exhibited for the dry monsoon season

FIGURE 6 (A) Percentage change (compared with a 1961–1990 baseline) in monsoon precipitation; (B) change in average annual surface air temperature in 3 QUMP experiments in 3 time periods.
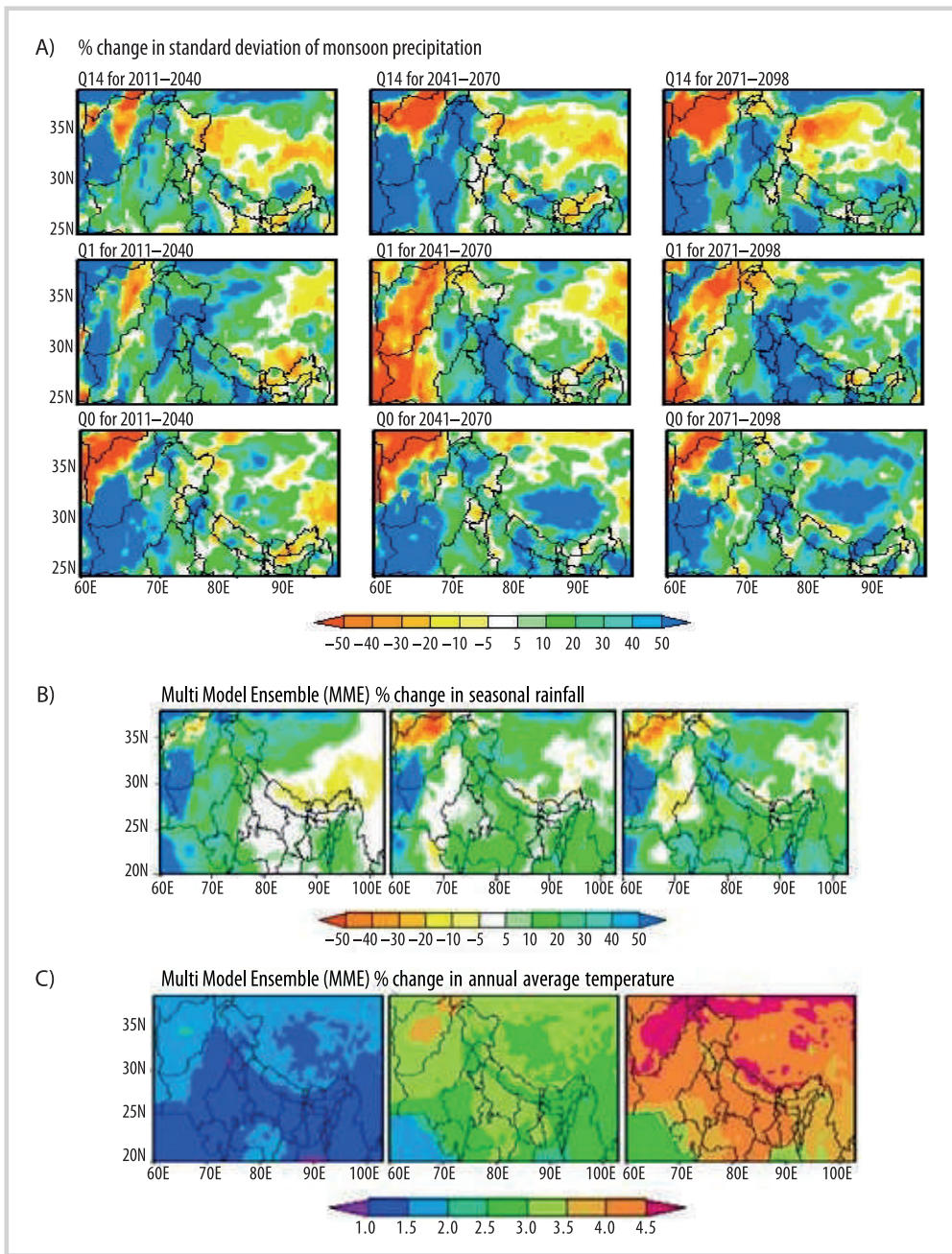

(November–March). During the monsoon season (June–September), the rainfall was simulated reasonably well. For the CH, Q1 tallied very well during the monsoon but exhibited a wet bias of 10–20 mm/mo in the remaining months. For the EH, a wet bias of 30–50 mm/mo was exhibited for the premonsoon months. Hence, there was a large uncertainty in the 3 simulations. However, in general, the model did reproduce the shape of the annual cycle of rainfall and surface air temperature reasonably well. The mode of precipitation seasonality in the WH is

during the winter months, and the primary hydrological impacts there from precipitation change will most likely be due to changes in winter rather than summer and monsoon precipitation.

The spatial patterns of seasonal rainfall as simulated by the 3 QUMP runs for the baseline period 1961–1990 were compared with the observed APHRODITE precipitation patterns, as shown in Figure 5A. PRECIS seems to provide an adequate representation of present-day conditions. The seasonal (June–September) rainfall

FIGURE 7 (A) Percentage changes in standard deviation of monsoon precipitation in 3 QUMP experiments for 3 time periods with respect to 1961–1990; (B) ensemble average of percentage change in seasonal rainfall; (C) ensemble average of change in annual average surface air temperature (°C) for 3 time periods with respect to 1961–1990.

TABLE 1 Ensemble mean summer monsoon rainfall (mm) and mean annual surface air temperature (°C) for 1961–1990, 2011–2040, 2041–2070, and 2071–2098 compared with observed values in the WH, CH, and EH. (Table extended on next page.)

Region	Summer monsoon rainfall (mm)				
	Observed	1961–1990	2011–2040	2041–2070	2071–2098
WH	86	97	114	106	105
CH	546	692	717	785	855
EH	1042	1130	1140	1204	1270

pattern was well simulated for the HKH region, as seen in Figure 5A. All the 3 QUMP runs exhibited a wet bias in the northern parts of the CH. Q0 and Q14 captured the seasonal rainfall amount and patterns quite reasonably, but Q1 exhibited a dry bias for the WH and some parts of the CH, which has also been seen for the Indian landmass (Krishna Kumar et al 2011).

The composite spatial patterns of annual average temperatures for 1961–1990 are given in Figure 5B. The cooler temperatures in the northern parts and warmer temperatures in southern parts of the HKH region were well simulated by all 3 experiments. All three exhibited a warm bias of 1–2°C in the EH. Cooler temperatures were simulated in the far northern tip of the WH.

Projected changes in rainfall and temperature

Projected percentage changes in seasonal rainfall in 3 QUMP simulations from the baseline (1961–1990) to the near future (2011–2040), the middle of the century (2041–2070), and the end of the century (2071–2098) are depicted in Figure 6A. Key projections were that the monsoon rainfall may decrease over the CH during 2011–2040, whereas there may be a 5–10% increase in rainfall in the WH and EH. In 2041–2070, rainfall may accelerate, but the northern parts of the CH may be deprived of rainfall. In 2071–2098, all 3 experiments project a 20–40% increase in seasonal rainfall for the entire HKH region. Because precipitation seasonality in the WH is during the winter months, the primary hydrological impacts there from precipitation change will most likely be due to changes in winter rather than summer and monsoon precipitation. There was a large discrepancy in the 3 projections of summer monsoon rainfall in the WH.

The projected changes in the surface air temperature for the same time frames and the QUMP runs are shown in Figure 6B. As time passes, the temperature is projected to rise by 0.5°C to more than 5°C. The maximum warming is projected for the WH. Q14 projects maximum warming for the HKH region. For 2011–2040, the warming is projected to be 0.5–1°C; for 2041–2070, 1–3°C; and for 2071–2098, 4–5°C, which would be quite threatening to the snow and glaciers throughout the region.

The possible percentage changes in standard deviation of summer monsoon rainfall under the 3 QUMP simulations for the 3 time periods are shown in Figure 7A. Monsoon rainfall was projected by all 3 QUMP simulations to be much more variable (a 20–40% rise in standard deviation) in the CH and EH toward the end of the century than it was in 1961–1990; a smaller change in variability (not more than 10%) was projected for the WH.

There is a large uncertainty in simulation by the 3 QUMP runs, and the best solution is to consider an ensemble average of the 3 runs (ie the average of projected changes given by the 3 QUMP simulations at every grid point). The ensemble projected changes in seasonal rainfall and annual average temperatures for the 3 time periods are also shown in Figure 7B and C, respectively. For 2011–2040, rainfall was projected to decrease over the CH and EH; during 2041–2070 there may be a 5–20% change, whereas, at the end of the century, there may be an increase of 20–40% in the CH and EH over 1961–1990 rainfall levels. Similarly, the annual average temperature is projected to rise in 2011–2040 by 1–2°C, in 2041–2070 by 1–3°C, and in 2071–2098 by 3–5°C for the HKH region. The rise in mean annual temperature may be greater in WH than in CH and EH, as seen in Figure 7. This may be a serious threat to the glaciers and snow cover in the HKH region. The ensemble mean values of the 3 QUMP runs are given in Table 1. All runs exhibited a wet bias for all 3 regions, but the mean annual temperatures were reasonably well simulated by the ensemble mean.

Conclusions

This study examined the variability and change in seasonal precipitation and annual average temperature in the HKH region as revealed by high-resolution gridded observed data as well as simulations under the PRECIS regional climate model. The main findings were as follows:

- All 3 QUMP simulations captured the annual cycle of surface air temperature in the HKH region reasonably well; however, they exhibited a warm bias of 3–4°C in the WH during the monsoon season.
- Although the shape of the annual cycle of precipitation in all 3 regions was well simulated, a wet bias was exhibited for the WH for the dry monsoon season (February–April) and for the CH for the monsoon

TABLE 1 Extended. (First page of Table 1 on previous page.)

Region	Mean annual temperature (°C)				
	Observed	1961–1990	2011–2040	2041–2070	2071–2098
WH	9.9	7.9	9.6	11.2	12.5
CH	8.9	9.2	10.8	12.4	13.5
EH	13.6	15.1	16.5	18.0	19.2

season. The rainfall maximum was simulated two months early (in May and June) for the EH.

- The spatial climatology of annual average temperature and monsoon rainfall were well simulated by all three QUMP runs.
- At the end of the century, the annual average temperature is projected to increase by 4–5°C, whereas rainfall may increase by 20–40% in the HKH region.
- Rainfall may be 40–50% more variable in the CH and EH at the end of the century.
- The ensemble mean of the 3 QUMP runs exhibited a wet bias over the WH and CH, and a dry bias over the

EH. It exhibited a warm bias for the CH and EH for mean annual temperatures.

Although the scenarios presented in this article are indicative of the expected range of rainfall and temperature changes, there are still large uncertainties associated with the quantitative estimates. Hence, the scenarios may be used only qualitatively and with caution, that is, the direction of change (decrease or increase) of impacts can be considered but actual figures given for projected changes should not be used because they involve uncertainty.

REFERENCES

Bolch T, Kulkarni A, Kääb A, Huggel C, Paul F, Cogley JG, Frey H, Kargel JS, Fujita K, Scheel M, Bajracharya S, Stoffel M. 2012. The state and fate of Himalayan glaciers. *Science* 336:310–314.
Collins M, Booth BBB, Harris GR, Murphy JM, Sexton DMH, Webb MJ. 2006. Towards quantifying uncertainty in transient climate change. *Climate Dynamics* 27:127–147.
Du MY, Kawashima S, Younemura S, Zhang XZ, Chen SB. 2004. Mutual influence between human activities and climate change in the Tibetan plateau during recent years. *Global Planetary Change* 41:241–249.
Dyurgerov MD, Meier MF. 2005. *Glaciers and Changing Earth System: A 2004 Snapshot*. Boulder, CO: Institute of Arctic and Alpine Research, University of Colorado.
Forsythe N, Kilsby CG, Fowler HJ, Archer DR. 2012. Assessment of runoff sensitivity in the Upper Indus Basin to interannual climate variability and potential change using MODIS satellite data products. *Mountain Research and Development* 32(1):16–29.
Fowler HJ, Archer DR. 2006. Conflicting signals of climate change in the Upper Indus basin. *Journal of Climate* 19:4276–4293.
Fujita K, Nakawo M, Fujii Y, Paudyal P. 1997. Changes in glaciers in Hidden Valley, Mukut Himal, Nepal Himalayas, from 1974 to 1994. *Journal of Glaciology* 43:583–588.
Grabs WE, Pokhrel AP. 1992. Establishment of measuring service for snow and glacier hydrology in Nepal: Conceptual and operational aspects. *In:* Young GJ, editor. *International Symposium on Snow and Glacier Hydrology*. Kathmandu, Nepal: International Association of Hydrological Sciences, pp 3–16.
IPCC [Intergovernmental Panel on Climate Change]. 2001. *Special Report: Emissions Scenarios. Summary for Policymakers*. www.ipcc.ch/pdf/special-reports/spm/sres-en.pdf; accessed on 27 December 2011.
IPCC [Intergovernmental Panel on Climate Change]. 2007. *Climate Change 2007: The Physical Sciences Basis*. Contribution of Working Group I to the Fourth Assessment Report of the IPCC. Cambridge: Cambridge University Press. www.ipcc.ch/pdf/assessment-report/ar4/wg1/ar4-wg1-frontmatter.pdf; accessed on 27 December 2011.
Jacob T, Wahr J, Tad Pfeffer W, Swenson S. 2012. Recent contributions of glaciers and ice caps to sea level rise. *Nature* 482:514–518.
Jones RG, Noguer M, Hassell DC, Hudson D, Wilson SS, Jenkins GJ, Mitchell JFB. 2004. *Generating High Resolution Climate Change Scenarios Using PRECIS*. Exeter, United Kingdom: Met Office Hadley Centre.
Kalnay E, Kanamitsu M, Kistler R, Collins W, Deaven D, Gandin L, Iredell M, Saha S, White G, Woollen J, Zhu Y, Leetmaa A, Reynolds R, Chelliah M, Ebisuzaki W. 1996. The NCEP/NCAR 40-year reanalysis project. *Bulletin of the American Meteorological Society* 77:437–471.

Krishna Kumar K, Patwardhan SK, Kulkarni A, Kamala K, Koteswara Rao K, Jones R. 2011. Simulation and future projections of summer monsoon climate over India by a high-resolution regional climate model (PRECIS). *Current Science* 101:312–326.
Mann HB. 1945. Nonparametric tests against trend. *Econometrica* 13:245–259.
Murphy JM, Sexton DMH, Barnett DN, Jones GS, Webb MJ, Collins M, Stainforth DA. 2004. Quantification of modelling uncertainties in a large ensemble of climate change simulations. *Nature* 430:768–772.
Patwardhan SK. 2012. *Study of the Impact of Climate Change on the Characteristics of Indian Summer Monsoon Using Regional Climate Model* [PhD dissertation]. Maharashtra, India: University of Pune.
Shrestha AB, Devkota LP. 2010. *Climate Change in the Eastern Himalayas: Observed Trends and Model Projections: Climate Change Impact and Vulnerability in the Eastern Himalayas – Technical Report 1*. Kathmandu, Nepal: International Centre for Integrated Mountain Development.
Shrestha AB, Wake CP, Mayewski PA, Dibb JE. 1999. Maximum temperature trends in the Himalaya and its vicinity: An analysis based on the temperature records from Nepal for the period 1971–94. *Journal of Climate* 12(9):2775–2786.
Sohn SJ, Tam C-Y, Ashok K, Ahn JB. 2011. Quantifying the reliability of precipitation datasets for monitoring large-scale East Asian precipitation variations. *International Journal of Climatology.* http://dx.10.1002/joc.2380.
Stainforth DA, Aina T, Christensen C, Collins M, Faull N, Frame DJ, Kettleborough JA, Knight S, Martin A, Murphy JM, Piani C, Sexton D, Smith LA, Spicer RA, Thorpe AJ, Allen MR. 2005. Uncertainty in predictions of the climate response to rising levels of greenhouse gases. *Nature* 433:403–406.
Xu J, Grumbine RE, Shrestha AB, Eriksson M, Yang X, Wang Y, Wilkes A. 2009. The melting Himalayas: Cascading effects of climate change on water, biodiversity, and livelihoods. *Conservation Biology* 23:520–530.
Yao T, Thompson L, Yang W, Yu W, Gao Y, Guo X, Yang X, Duan K, Zhao H, Xu B, Pu J, Lu A, Xiang Y, Kattel DB, Joswiak D. 2012. Different glacier status with atmospheric circulations in Tibetan Plateau and surroundings. *Nature Climate Change* 2:663–667.
Yatagai A, Arakawa O, Kamiguchi K, Kawamoto H, Nodzu M, Hamada A. 2009. A 44-year daily gridded precipitation dataset for Asia based on a dense network of rain gauges. *Scientific Online Letters on the Atmosphere* 5:137–140.
Yatagai A, Kamiguchi K, Arakawa O, Hamada A, Yasutomi N, Kitoh A. 2012. APHRODITE: Constructing a long-term daily gridded precipitation dataset for Asia based on a dense network of rain gauges. *Bulletin of the American Meteorological Society* 93:1401–1415.